

## Relaxation dynamics of lithium ions in lead bismuthate glasses

A. Pan and A. Ghosh

*Department of Solid State Physics, Indian Association for the Cultivation of Science, Jadavpur, Calcutta 700032, India*

(Received 27 January 2000)

We have investigated relaxation dynamics of lithium ions in lead bismuthate glasses in the frequency range from 10 Hz to 2 MHz and in the temperature range from 303–553 K. Using the Anderson-Stuart model, we have calculated the activation energy, which is observed to be lower than that of the dc conductivity. We have studied the relaxation mechanism of these glasses in the framework of the electric modulus and conductivity formalisms. The microscopic parameters obtained from these formalisms have been compared. We have also calculated the decoupling index and correlated them with the stretched exponential relaxation parameter and the dc conductivity.

### I. INTRODUCTION

Over the past few years there has been renewed interest in the investigation of glasses that have ions as the primary charge carriers and can find their applications as solid-state electrolytes. Several efforts<sup>1–3</sup> in this regard have been devoted to predict the electrical transport properties and design ion conducting glasses. In order to design the desired glasses, the correlation between the electrical properties and the structure must be understood properly. However, there are few reports<sup>4</sup> on the structure of these glasses. Moreover, the above studies remain confined to glasses formed with traditional glass formers like SiO<sub>2</sub>, P<sub>2</sub>O<sub>5</sub>, B<sub>2</sub>O<sub>3</sub>, etc.<sup>5</sup> Glasses formed with heavy metal oxides such as TeO<sub>2</sub>, Bi<sub>2</sub>O<sub>3</sub>, and PbO remain almost ignored.<sup>6</sup> The structural studies<sup>7</sup> of some bismuthate and lead bismuthate glasses reveal the presence of distorted BiO<sub>5</sub>-BiO<sub>6</sub> and PbO<sub>3</sub>-PbO<sub>4</sub> polyhedra as the main structural units. At lower Li<sub>2</sub>O content, Li<sup>+</sup> ions go into the structural interstices to compensate the excess negative charge of BiO<sub>5</sub>-BiO<sub>6</sub> polyhedra. At higher Li<sub>2</sub>O content, however, the charge compensation is exceeded and a few of the relatively strong Bi-O bonds are replaced by weak Li<sup>+</sup>O<sup>-</sup> bonds. It has been shown that the introduction of PbO influences the structure of these glasses as PbO may act as a modifier as well as a glass former.<sup>8</sup>

Although considerable efforts<sup>9–13</sup> have been made to explore the ionic conductivity and relaxation mechanisms in ionic glasses, the understanding of the mechanism for the conductivity still remains unclear because of the difficulty in separating the contribution of ionic concentration and mobility from the total measured conductivity. The contribution of the ionic concentration on the relaxation mechanism also remains unresolved.<sup>14,15</sup> In general, two formalisms, namely, the conductivity and the electric modulus, have been followed to study the relaxation processes.<sup>16,17</sup> However, it has not been resolved which of them can describe the relaxation process better.

In the present paper, we have studied the conductivity and relaxation mechanism in lithium lead bismuthate glasses. The dc conductivity has been calculated using the Anderson-Stuart model and compared with the experimental values. The ac conductivity has been analyzed in the framework of both the electric modulus and the conductivity formalisms. In the former technique the stretched exponential Kohlrausch-Williams-Watts (KWW) function has been used

to account for the non-Debye relaxation. The latter technique has been used to determine the microscopic parameters, namely, the hopping frequency, the activation energy for creation and migration separately, the effective concentration of charge carriers, and the frequency exponent. These microscopic parameters have been compared with those obtained from the modulus formalism.

### II. EXPERIMENTAL PROCEDURE

The lithium lead bismuthate glasses of compositions  $x\text{Li}_2\text{O}-(100-x) [\text{Bi}_2\text{O}_3\text{-PbO}]$ , where  $x=20, 30, 40, 50$ , and 60 mol %, were prepared by a melt-quenching method. Appropriate amounts of reagent grade chemicals Bi<sub>2</sub>O<sub>3</sub>, PbO, and Li<sub>2</sub>CO<sub>3</sub> (Aldrich, 99+%) were thoroughly mixed and decarbonized at 450 °C for 2 h. The mixtures were then melted in alumina crucibles. The melts were equilibrated for about 1 h at 800–1000 °C (depending on the composition) in air in an electrical furnace. Glassy samples were obtained either by pressing the melts in between two copper plates or by pouring them in a twin roller. The samples were annealed in another furnace maintained at 200 °C to remove residual stresses. All the samples were transparent and yellow in color. The glassy nature of the samples was confirmed from the x-ray diffraction patterns recorded in an x-ray diffractometer (Seifert, model-3000P). Glass transition temperatures ( $T_g$ ) of the samples were determined using a differential thermal analyzer (Shimadzu, model DT-40). The density was measured at room temperature by liquid displacement method using acetone as the immersion liquid. Gold electrodes were deposited on both the surfaces of the prepared samples of thickness ~0.02–0.05 cm and diameter ~1.5 cm. Electrical measurements such as capacitance and conductance of the samples were carried out using a precision RLC bridge (QuadTech, model 7600) in the temperature range 303–553 K and in the frequency range 10 Hz–2 MHz. The dc conductivity of the samples was determined from the complex impedance plots.

### III. RESULTS AND DISCUSSION

#### A. dc conductivity

We have shown in Fig. 1 the dc conductivity for all the glass compositions as a function of reciprocal temperature. All the plots are linear, indicating thermally activated hop-

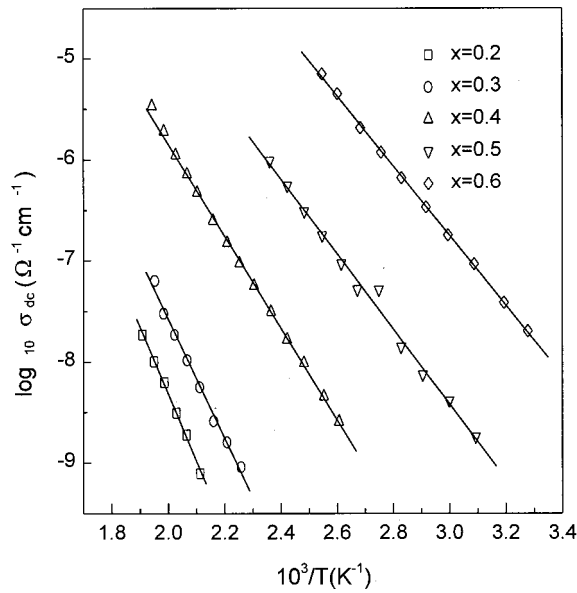


FIG. 1. dc conductivity shown as a function of reciprocal temperature for all compositions of  $x\text{Li}_2\text{O}-(100-x)[\text{PbO}-\text{Bi}_2\text{O}_3]$  glasses shown in the inset. The solid lines are the least-squares straight-line fits.

ping conductivity. The activation energy for different compositions was obtained from the least-squares straight-line fits and is shown in Table I. We have presented in Figs. 2(a) and 2(b) a comparison of the dc conductivity at 200 °C and the activation energy, respectively, of the present lithium lead bismuthate glasses with those of glasses formed with other glass formers such as borate<sup>18</sup> and bismuthate.<sup>6</sup> It is noted that the conductivity of the  $\text{Li}_2\text{O}-\text{Bi}_2\text{O}_3-\text{PbO}$  glasses is higher than that of the  $\text{Li}_2\text{O}-\text{Bi}_2\text{O}_3$  glasses for higher  $\text{Li}_2\text{O}$  content ( $\geq 40$  mol %). Structural studies<sup>7</sup> of lead bismuthate glasses indicate that most of the  $\text{Li}^+$  ions for the glasses with lower  $\text{Li}_2\text{O}$  content coordinate with the  $\text{BiO}_5$  and  $\text{BiO}_6$  polyhedra by breaking Bi-O-Bi bonds, as the coordination number of Bi is greater than that of Pb. Thus the conductivity for these compositions of the  $\text{Li}_2\text{O}-\text{Bi}_2\text{O}_3-\text{PbO}$  glasses agrees fairly well with that of the  $\text{Li}_2\text{O}-\text{Bi}_2\text{O}_3$  glasses. But when the  $\text{Li}_2\text{O}$  content exceeds 40 mol %, a fraction of the  $\text{Li}^+$  ions coordinates with the  $\text{PbO}_3$  polyhedra through the weak  $\text{Pb}-\text{O}^--\text{Li}^+$  bonds, which leads to the enhancement of the conductivity in the glasses with higher  $\text{Li}_2\text{O}$  content. We also note in Fig. 2(a) a steep rise in the conductivity in the low alkali region of borate glasses, which is attributed to the

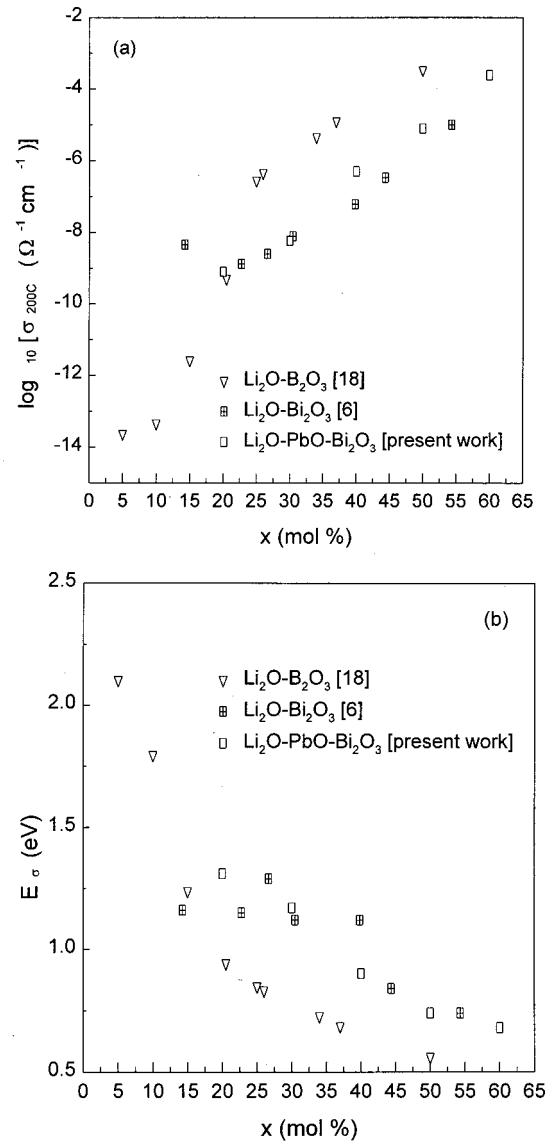


FIG. 2. (a) Comparison of the dc conductivity at 200 °C and (b) the dc activation energy of lithium lead bismuthate glasses with that of lithium borate (Ref. 18), and lithium bismuthate (Ref. 6) glasses.

structural transformation occurring due to the introduction of  $\text{Li}_2\text{O}$ .<sup>18,19</sup> At higher  $\text{Li}_2\text{O}$  content, the conductivity for these glasses becomes less composition dependent as no major structural transformation takes place in this composition range.<sup>19</sup>

TABLE I. The activation energy for dc conductivity, binding energy, strain energy, deviation from the total activation energy, activation energy for relaxation, high-frequency dielectric constant, and the stretched exponential parameter for  $x\text{Li}_2\text{O}-(100-x)[\text{PbO}-\text{Bi}_2\text{O}_3]$  glass.

Composition $x$ (mol %)	$E_\sigma$ (eV) ( $\pm 0.01$ )	$E_B$ (eV)	$E_S$ (eV)	$E_P$ $= E_\sigma - (E_B + E_S)$ (eV)	$E_\tau$ (eV) ( $\pm 0.02$ )	$\epsilon_\infty$	$\beta$ ( $\pm 0.02$ )
20	1.31	0.13	0.65	0.53	1.58	34.5	0.63
30	1.17	0.10	0.38	0.69	1.26	29.4	0.56
40	0.90	0.09	0.32	0.49	0.89	26.3	0.54
50	0.74	0.12	0.39	0.23	0.73	19.6	0.52
60	0.68	0.09	0.32	0.27	0.68	20.8	0.56

We have calculated the activation energy using the Anderson and Stuart model.<sup>20</sup> In this model, the total activation energy ( $E_\sigma$ ) consist of two terms: the electrostatic binding energy ( $E_B$ ) required to remove a cation from a nonbridging oxygen site and the strain energy ( $E_S$ ) required to dilate the structure as the ion moves from one site to another. Thus the total activation energy in this model can be written as<sup>20</sup>

$$E_\sigma = E_B + E_S, \quad (1)$$

where the binding energy is given by

$$E_B \approx ZZ_0 e^2 [1/(r+r_0) - 2/\lambda] / \epsilon_\infty \quad (2)$$

and the strain energy term modified by McElfresh and Howitt<sup>21</sup> is given by

$$E_S = \pi\lambda G(r-r_D)^2/2. \quad (3)$$

The terms  $Z$ ,  $Z_0$  and  $r$ ,  $r_0$  are the charges and radii of the cation and nonbridging oxygen, respectively,  $\epsilon_\infty$  is the high-frequency dielectric constant,  $r_D$  is the doorway radius,  $\lambda$  and  $G$  being the effective hop distance between the cation sites and the shear modulus, respectively.

We have calculated the values of  $E_B$  and  $E_S$  separately by using the values of  $\epsilon_\infty$  (Table I) estimated from the electric modulus plots and by assuming the hop distance as the effective cation-cation distance. The values of the shear modulus have been obtained from the acoustic measurements and the doorway radius is assumed to be 0.17 Å equal to that of borate glasses. The calculated values are presented in Table I, which reveals that the activation energy for different compositions obtained from the conductivity measurements is higher than the sum of  $E_B$  and  $E_S$ . This discrepancy can be understood by considering Eq. (2) and the values of the high-frequency dielectric constant that actually scales down the binding energy  $E_B$ . The high values of  $\epsilon_\infty$  for the lead bismuthate glasses arise from the contribution of the network forming bismuth and lead ions, which is quite evident from their compositional variation (Table I). But for the calculation of the binding energy of the network modifier ion, only the dielectric constant arising from the nonbridging oxygen-network modifier ionic bonds needs to be taken into account. However, what we get here from the electric modulus plots is the total dielectric constant, which contains the contribution of both the ionic bond as well as the polarizability of the heavy metal network former ions. In terms of the energetic of the Anderson-Stuart model<sup>20</sup> in the configuration coordinate diagram, the presence of heavy metal network former deepens the potential well in spite of the enhancement of the overall dielectric constant.<sup>22</sup>

### B. ac conductivity

We have analyzed the relaxation dynamics of lithium ions in lead bismuthate glasses in the framework of conductivity and modulus formalisms. In the modulus formalism,<sup>17</sup> an electric modulus  $M^*(\omega)$  is defined as the reciprocal of complex dielectric permittivity  $\epsilon^*(\omega)$  by

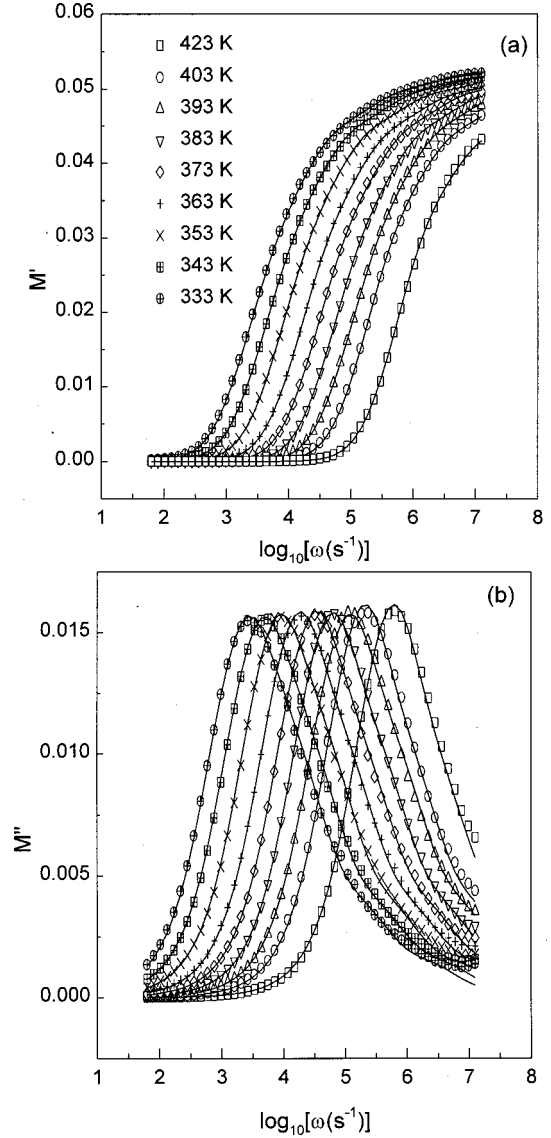


FIG. 3. Frequency dependence of (a) real and (b) imaginary parts of modulus isotherms of 50Li<sub>2</sub>O-50[PbO-Bi<sub>2</sub>O<sub>3</sub>] glass. The solid lines are the best fits to Eq. (4).

$$M^*(\omega) = 1/\epsilon^*(\omega) = M'(\omega) + iM''(\omega) = M_\infty \times \left[ 1 - \int_0^\infty \exp(-i\omega t) \{-d\phi(t)/dt\} dt \right], \quad (4)$$

where  $M_\infty = 1/\epsilon_\infty$ ,  $\epsilon_\infty$  is the high-frequency asymptotic value of the real part of the dielectric constant, and  $\phi(t)$  is the relaxation function, which evolves the electric field within the material. The relaxation function in our case is taken as the KWW function<sup>23</sup> given by

$$\phi(t) = \exp\{-(t/\tau_m)^\beta\}, \quad (5)$$

where  $\beta$  measures the extent of the nonexponentiality. Figures 3(a) and 3(b) show the frequency dependence of the real and imaginary parts of the modulus spectra, respectively, at different temperatures for a glass composition (50Li<sub>2</sub>O-50[Bi<sub>2</sub>O<sub>3</sub>-PbO]). The real part of the electric modulus  $M'(\omega)$  exhibits very small values at lower frequencies revealing the ease of migration of the conducting ions. As

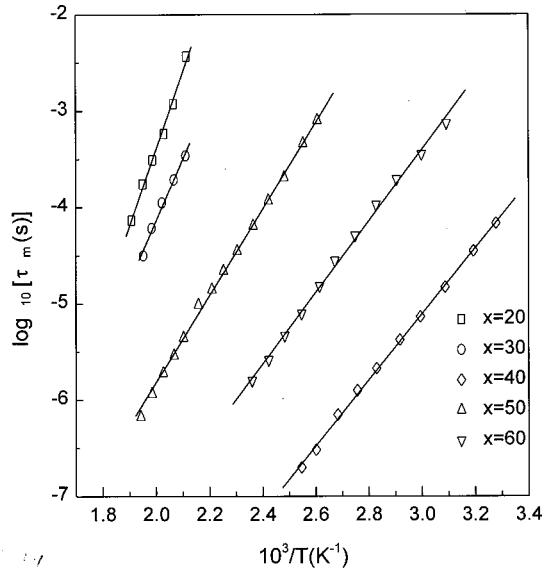


FIG. 4. Reciprocal temperature dependence of the conductivity relaxation times for different compositions of  $x\text{Li}_2\text{O}-(100-x)\text{[PbO-Bi}_2\text{O}_3]$  glasses shown in the inset. The solid lines are the least-squares straight-line fits to the data.

the frequency of the applied field is increased,  $M'(\omega)$  shows a dispersion tending to  $M_\infty$  at higher frequencies. The imaginary part of the electric modulus  $M''(\omega)$  shows an asymmetric maximum at frequency  $\omega_m$  centered at the dispersion region of  $M'(\omega)$ . The frequency corresponding to the peak of  $M''(\omega)$  gives the most probable conductivity relaxation time  $\tau_m$  by the condition  $\omega_m \tau_m = 1$ . We have shown in Fig. 4 the reciprocal temperature dependence of the conductivity relaxation time that obeys the Arrhenius relation  $\tau_m = \tau_0 \exp(E_r/kT)$ . The activation energy  $E_r$  for the relaxation process (Table I) obtained from the least-squares straight-line fits is close to the activation energy for the conductivity for higher  $\text{Li}_2\text{O}$  content, consistent with the fluctuation dissipation theorem.<sup>24</sup> The discrepancy at lower  $\text{Li}_2\text{O}$  content is not clear at present. We have shown in Fig. 5 a master plot

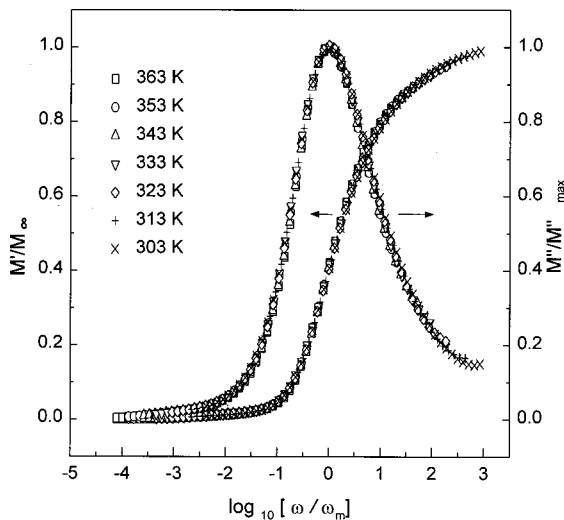


FIG. 5. Master plot of the electric modulus of  $60\text{Li}_2\text{O}-40[\text{PbO-Bi}_2\text{O}_3]$  glass for all temperatures shown in the inset.

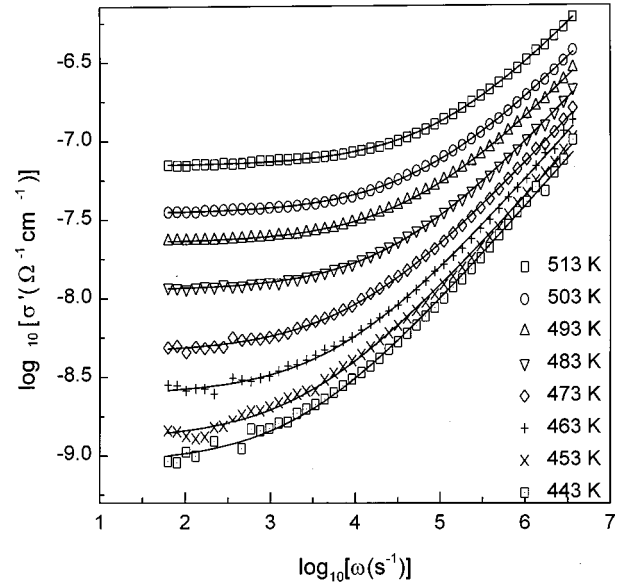


FIG. 6. Conductivity isotherms of  $30\text{Li}_2\text{O}-70[\text{PbO-Bi}_2\text{O}_3]$  glass as a function of frequency. The solid curves are the best fits to Eq. (7).

for the electric modulus in which each frequency is scaled by the peak frequency ( $\omega_m$ ) and  $M'(M'')$  is scaled by  $M_\infty(M''_{\text{max}})$ . We note that all the curves for different temperatures overlap on a single master curve that indicates temperature independence of the dynamical processes. The data in Figs. 3(a) and 3(b) were fitted to Eqs. (4) and (5) to obtain the values of the stretched exponential parameter  $\beta$  and the high-frequency dielectric constant (Table I). It may be noted that the values of  $\beta$  remain almost constant in the higher composition region as there occurs no structural change. But for lower  $\text{Li}_2\text{O}$  content, the values of  $\beta$  increase indicating that the interaction between the charge carriers decreases due to the structural transformation that occurs by replacing the Bi-O bonds of the  $\text{BiO}_5$  and  $\text{BiO}_6$  polyhedra and Pb-O bonds of  $\text{PbO}_3$  and  $\text{PbO}_4$  polyhedra, which can accommodate the  $\text{Li}^+$  ions.

We have also studied the dynamics of the  $\text{Li}^+$  ions in the lead bismuthate glasses in the framework of the conductivity formalism proposed by Almond, Duncan and West.<sup>16</sup> In this formalism the real part of the frequency-dependent conductivity  $\sigma'(\omega)$  is expressed by

$$\sigma'(\omega) = \sigma_{\text{dc}} [1 + (\omega/\omega_H)^n], \quad (6)$$

TABLE II. Creation energies, migration energies, total activation energy, and the frequency exponent obtained from the conductivity formalism for  $x\text{Li}_2\text{O}-(100-x)\text{[PbO-Bi}_2\text{O}_3]$  glasses.

Composition $x(\text{mol } \%)$	$\Delta E_c$ (eV) ( $\pm 0.01$ )	$\Delta E_m$ (eV) ( $\pm 0.01$ )	$E_a$ (eV) $= \Delta E_c + \Delta E_m$	$n$ ( $\pm 0.02$ )
20	0.57	1.00	1.57	0.78
30	0.38	1.18	1.56	0.60
40	0.08	0.87	0.95	0.62
50	0.05	0.76	0.81	0.62
60	0.02	0.70	0.72	0.61

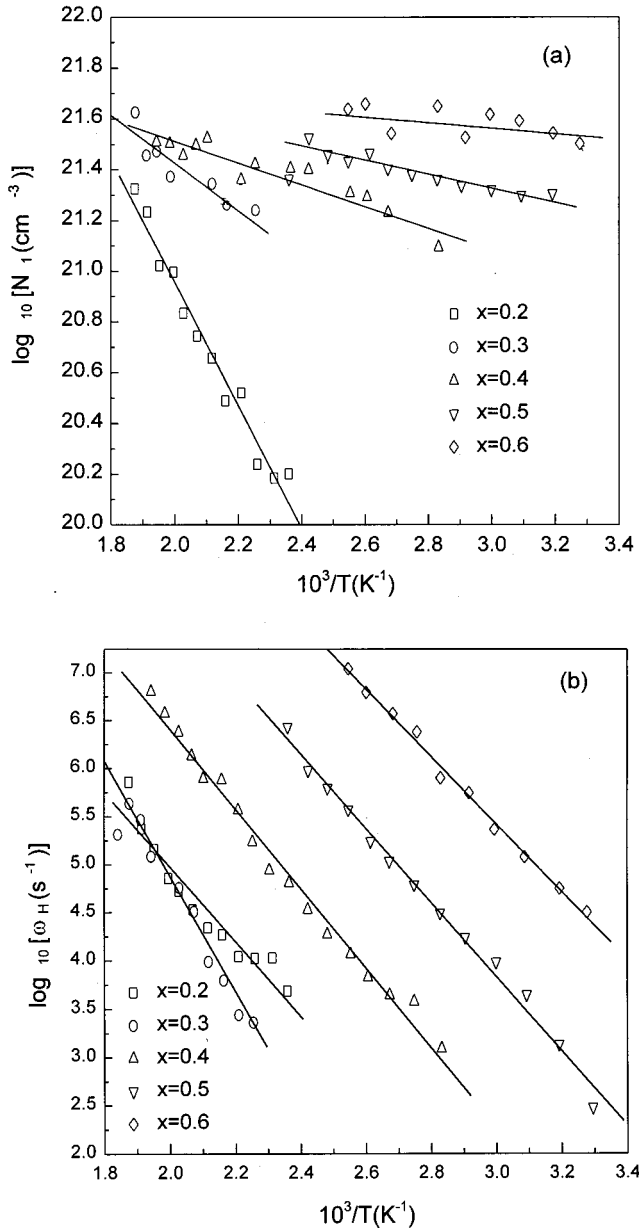


FIG. 7. (a) Charge carrier concentration and (b) hopping frequency for  $x\text{Li}_2\text{O}-(100-x)[\text{PbO}-\text{Bi}_2\text{O}_3]$  glasses shown as a function of reciprocal temperature. The solid lines are the least-squares straight-line fits.

where  $\omega_H$  is the hopping frequency of the charge carriers and  $n$  ( $0 \leq n \leq 1$ ) is the frequency exponent, which measures the interaction between the mobile ions. Assuming thermally activated charge carriers and hopping frequencies with activation energies  $\Delta E_c$  and  $\Delta E_m$ , respectively, and using the Nernst-Einstein relation for  $\sigma_{dc}$ , Eq. (6) can be written as

$$\begin{aligned} \sigma(\omega) &= N_0(Ze)^2 \gamma \lambda^2 \omega_0 \exp[-(\Delta E_c + \Delta E_m)/kT] [1 \\ &\quad + \{\omega/\omega_0 \exp(\Delta E_m/kT)\}^n] / 2\pi kT \\ &= N_1(Ze)^2 \gamma \lambda^2 \omega_H [1 + (\omega/\omega_H)^n] / 2\pi kT, \end{aligned} \quad (7)$$

where  $N_1$  is the effective concentration of charge carriers,  $e$  the electronic charge,  $\gamma$  the geometrical factor for ionic hopping and is  $\frac{1}{6}$  for isotropic glass,  $\lambda$  the average jump distance

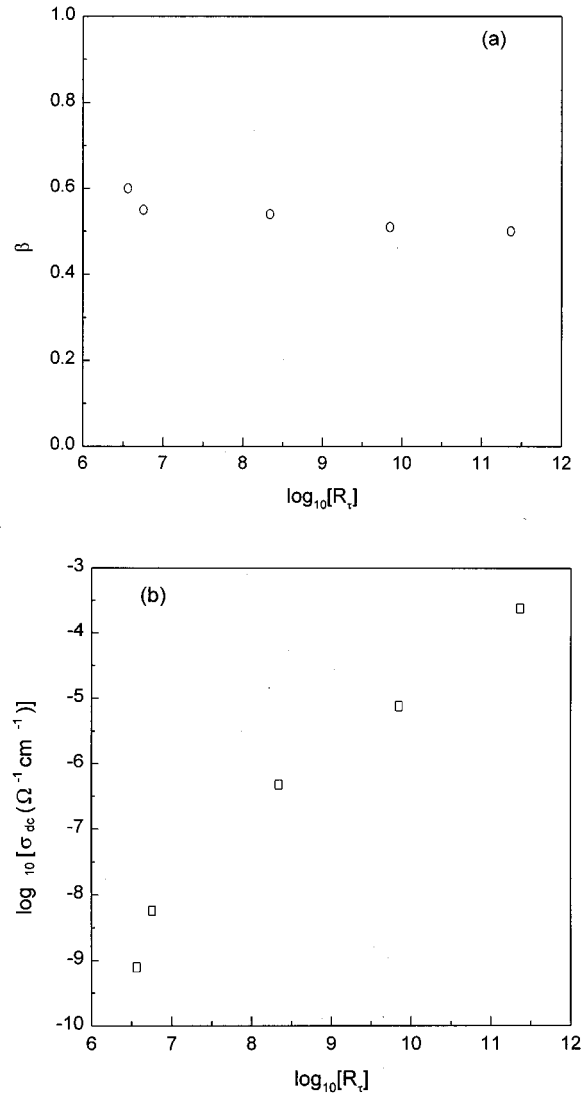


FIG. 8. (a) Correlation of the stretched exponential parameter  $\beta$  and (b) the dc conductivity with the decoupling index for  $x\text{Li}_2\text{O}-(100-x)[\text{PbO}-\text{Bi}_2\text{O}_3]$  glasses.

between the mobile ion sites. In the present calculation we have assumed the ion jump distance to be equal to average cation-cation separation distance ( $R$ ).

The conductivity data at different temperatures have been fitted to Eq. (7) using  $N_1$ ,  $\omega_H$ , and  $n$  as variable parameters. Such a fit is shown in Fig. 6 for a glass composition. The results of the analysis for all glass compositions are listed in Table II. It is interesting to note the temperature dependence of the concentration of charge carriers,  $N_1$  shown in Fig. 7(a). We note that the concentration of charge carriers depends on temperature for low  $\text{Li}_2\text{O}$  content. This result agrees with that of structural studies,<sup>7</sup> which suggest that at low  $\text{Li}_2\text{O}$  content the  $\text{Li}^+$  ions occupy the structural interstices of  $\text{BiO}_5$ - $\text{BiO}_6$  and  $\text{PbO}_3$ - $\text{PbO}_4$  polyhedra and are thermally activated with an energy of activation  $\Delta E_c$  and contribute to the conductivity within this composition range. At a higher  $\text{Li}_2\text{O}$  content region,  $\text{Li}^+$  ions are easily accessible in the presence of applied electric field to contribute to the conductivity at all temperatures and thus they are not thermally activated. Consequently, the creation energy should go

on decreasing with increasing alkali content as observed from the values of  $\Delta E_c$  (Table II), which was computed from the least-squares straight-line fits of the data in Fig. 7(a).

The reciprocal temperature dependence of hopping frequency ( $\omega_H$ ) obtained from the fits is also shown in Fig. 7(b), which exhibits an activated behavior with an activation energy for migration,  $\Delta E_m$ . The values of  $\Delta E_m$  are obtained from the least-squares straight-line fits of the data. The total activation energy for conduction ( $E_a$ ) has been obtained by adding the creation and migration energies. The values of  $E_a$  (Table II) obtained from this formalism agree fairly well with those obtained from the modulus formalism (Table I). We note that the frequency exponent  $n$  does not obey Ngai's relation<sup>24</sup>  $\beta = 1 - n$ . The difference arises from the fact that the single KWW function used for fitting the observed modulus spectra leaves the high-frequency component unaccounted,<sup>4</sup> which is evident from Fig. 3(b). The other reason might be the fact that the shape of the modulus spectra is influenced by the values of the high-frequency dielectric constant ( $\epsilon_\infty$ ) as pointed out by different authors.<sup>25,26</sup> In contrast, the conductivity formalism takes into account the high-frequency region of the conductivity spectra determined by the frequency exponent  $n$ .

We have calculated the extent of the decoupling between the diffusional motion of the mobile ion and the viscous motion of the host glassy network.<sup>27</sup> The decoupling index  $R_\tau$  was defined by Angell<sup>27</sup> as  $R_\tau = \langle \tau_s(T_g) \rangle / \langle \tau_m(T_g) \rangle$ , where  $\langle \tau_s(T_g) \rangle$  and  $\langle \tau_m(T_g) \rangle$  are the average values of the structural and conductivity relaxation times at the glass transition temperature  $T_g$ . The values of  $R_\tau$  were obtained by estimating the conductivity relaxation time at glass transition temperature  $\tau_m(T_g)$  from the extrapolated value (Fig. 4) and by assuming the structural relaxation time  $\tau_s(T_g) \sim 200$  s at the glass transition temperature. The correlation of the non-

exponentiality parameter  $\beta$  and the dc conductivity with the decoupling index is shown in Figs. 8(a) and 8(b), respectively. These figures reveal that the more the diffusive motion of the mobile species are decoupled from the viscous motion, the relaxation of the electric field becomes slower as the value of  $\beta$  becomes smaller consistent with Angell's interpretation of the decoupling index.

#### IV. CONCLUSIONS

Temperature-dependent conductivity and relaxation of lithium lead bismuthate glasses have been presented in the frequency range from 10 Hz to 2 MHz. The dc conductivity and activation energy of these glasses has been compared with those of borate and bismuthate glasses having  $\text{Li}_2\text{O}$  as modifier. The activation energy calculated from the Anderson-Stuart model is observed to be lower than the measured values due to high values of the dielectric constant. The analysis of the relaxation dynamics of the glasses has been made in the framework of the electric modulus as well as the conductivity formalisms. The microscopic parameters such as the hopping frequency, the activation energy, and the frequency exponent obtained from the analysis have been compared. It is noteworthy that for lower  $\text{Li}_2\text{O}$  content the concentration of the charge carriers shows an activated behavior. The decoupling index for the present glasses has been correlated with the stretched exponential parameter ( $\beta$ ) and the dc conductivity. The ions become more likely to correlate to each other's motion, as they become more and more decoupled from the viscous motion of the network.

#### ACKNOWLEDGMENT

One of the authors (A.P.) acknowledges the partial financial support of CSIR (India) for this work.

<sup>1</sup>D. L. Sidebottom, Phys. Rev. Lett. **83**, 983 (1999).

<sup>2</sup>K. L. Ngai, J. Chem. Phys. **110**, 10 576 (1999).

<sup>3</sup>J. Swenson and L. Borjesson, Phys. Rev. Lett. **77**, 3569 (1996).

<sup>4</sup>J. Wong and C. A. Angell, *Glass Structure by Spectroscopy* (Decker, New York, 1976).

<sup>5</sup>H. K. Patel and S. W. Martin, Phys. Rev. B **45**, 10 292 (1992), and references therein.

<sup>6</sup>A. Pan and A. Ghosh, Phys. Rev. B **60**, 3224 (1999); J. Chem. Phys. **112**, 1503 (2000).

<sup>7</sup>J. Fu, Phys. Chem. Glasses **37**, 84 (1996); Y. G. Choi, K. H. Kim, V. H. Chernov, and J. Heo, J. Non-Cryst. Solids **259**, 205 (1999).

<sup>8</sup>K. J. Rao, B. G. Rao, and S. R. Elliott, J. Mater. Sci. **20**, 1678 (1985).

<sup>9</sup>S. R. Elliott and A. P. Owen, Ber. Bunsenges. Phys. Chem. **95**, 987 (1991).

<sup>10</sup>A. Bunde, M. D. Ingram, and P. Maass, J. Non-Cryst. Solids **172-174**, 1222 (1994).

<sup>11</sup>P. Maass, M. Meyer, and A. Bunde, Phys. Rev. B **51**, 8164 (1995).

<sup>12</sup>K. L. Ngai, J. Non-Cryst. Solids **103**, 232 (1996).

<sup>13</sup>D. L. Sidebottom, P. F. Green, and R. K. Brow, J. Chem. Phys.

**108**, 5870 (1998).

<sup>14</sup>H. Jain and S. Krishnaswami, Solid State Ionics **105**, 129 (1998).

<sup>15</sup>B. Roling, A. Happe, K. Funke, and M. D. Ingram, Phys. Rev. Lett. **78**, 2160 (1997).

<sup>16</sup>D. P. Almond, G. K. Duncan, and A. R. West, Solid State Ionics **8**, 159 (1983); **9&10**, 277 (1983).

<sup>17</sup>P. B. Macedo, C. T. Moynihan, and R. Bose, Phys. Chem. Glasses **13**, 171 (1972).

<sup>18</sup>K. Otto, Phys. Chem. Glasses **7**, 29 (1966).

<sup>19</sup>J. Krogh-Moe, Phys. Chem. Glasses **6**, 46 (1965).

<sup>20</sup>O. L. Anderson and D. A. Stuart, J. Am. Ceram. Soc. **37**, 573 (1954).

<sup>21</sup>D. K. McElfresh and D. G. Howitt, J. Am. Ceram. Soc. **69**, C237 (1986).

<sup>22</sup>S. R. Elliott, *Physics of Amorphous Materials*, 2nd ed. (Longman, London, 1990), p. 249.

<sup>23</sup>G. Williams and D. C. Watts, Trans. Faraday Soc. **66**, 80 (1970).

<sup>24</sup>K. L. Ngai, Solid State Phys. **9**, 127 (1979).

<sup>25</sup>J. C. Dyre, J. Non-Cryst. Solids **135**, 219 (1991).

<sup>26</sup>B. Roling, Solid State Ionics **105**, 185 (1998).

<sup>27</sup>C. A. Angell, Chem. Rev. **90**, 523 (1990).